

Three body recombination of ultracold dipoles to weakly bound dimers.

Seth T. Rittenhouse¹ and Christopher Ticknor^{1,2,3}

¹*ITAMP, Harvard-Smithsonian Center for Astrophysics, Cambridge, Massachusetts 02138, USA*

²*ARC Centre of Excellence for Quantum-Atom Optics and Centre for Atom Optics and Ultrafast Spectroscopy, Swinburne University of Technology, Hawthorn, Victoria 3122, Australia*

³*Theoretical Division, Los Alamos National Laboratory, Los Alamos, New Mexico 87545, USA*

(Dated: October 18, 2018)

We use universality in two-body dipolar physics to study three-body recombination. We present results for the universal structure of weakly bound two-dipole states that depend only on the s-wave scattering length (a). We study threshold three-body recombination rates into weakly-bound dimer states as a function of the scattering length. A Fermi Golden rule analysis is used to estimate rates for different events mediated by the dipole-dipole interaction and a phenomenological contact interaction. The three-body recombination rate in the limit where $a \gg D$ contains terms which scale as a^4 , $a^2 D^2$ and D^4 , where D is the dipolar length. When $a \ll D$, the three-body recombination rate scales as D^4 .

PACS numbers: 34.20.Cf,34.50.-s,05.30.Fk

Universality has become increasingly important and applicable in ultracold physics. Two remarkable examples are: strongly interacting fermions [1–3] and few-body systems with large scattering lengths. Three-body recombination, $A + A + A \rightarrow A_2 + A + KE$, is of special interest in an ultracold gas. It usually is the limiting process determining the lifetime of the gas in the absence of two-body losses. Three-body recombination has also proven to be an important probe in understanding the basic quantum mechanical nature of universal few-body systems [4]. The experimental observation of universal 3- and 4-body loss features [5–7], associated with a class of three-body-bound state predicted by Efimov [8], is one of the major success stories in this field. These few-body complexes have found great utility because of the control over the two-body scattering length with a magnetic Fano-Feshbach resonance [9]. In a magnetic field, the last bound state can be tuned through the scattering threshold giving complete control over the scattering length. When a is much greater than the range of the short range interaction, many properties become independent of the details of the two-body interaction. For example, the three-body recombination takes on universal scaling behavior of a^4 in this regime [10].

The powerful idea of universality can be exploited to study complex systems. Now ultracold polar molecules have emerged [11, 12], and these systems will have a new type of collisional control [13]. This control emerges in the form of the dipole-dipole interaction, $V_{dd} = d^2[1 - 3(\hat{z} \cdot \hat{r})^2]/r^3$ where r is the inter-particle separation vector and d is the induced dipole moment along an external field axis (\hat{z}). The collisional control can be achieved through the induced dipole moment d which is determined by the strength of the electric field. As the electric field is increased, there is a series of s-wave dominated resonances [14–16]. These resonances occur when the system gains a weakly-bound long-range state. The short-range bound states structure of the interaction is largely independent of the external fields strength. These

threshold resonances could be used to control scattering length, but the importance of these resonances will go further. The interaction is a long range and anisotropic which will mediate fundamentally novel quantum behavior. What is striking about this interaction is that the length scale describing it can be incredibly large, many orders of magnitude larger than the short range interaction. The dipolar length scale is $D = \mu_{2b} d^2 / \hbar^2$ and μ_{2b} is the reduced mass of a two body system. This large length scale can be used to create a highly correlated system.

The two-dipole scattering cross section has been demonstrated to be universal [15, 17, 18]. In this work we extend the concept of universality in two-body dipolar physics and apply it to three-body recombination. We present results showing the universal structure of weakly bound two-dipole states that depend only on a . Using this, we then study threshold three-body recombination rates into weakly-bound dimer states as a function of a .

To start, we study the universality of the dipolar threshold resonances. These universal dipolar collisions depend only on the s-wave scattering length. To tune the scattering length, we vary the short range position of a hard wall boundary condition [15]. As the inner wall's position is decreased the system has a series of threshold resonances; in a real system this mimics increasing the electric field and the molecule's polarization. In this work we only study threshold resonances, the wide s-wave dominated resonances. There are other resonances which are not s-wave dominated, but these will be narrow and rare [15].

Examples of universal two-body scattering are well known, for instance when the scattering length is large and positive, large dimers form with binding energies $E_b = \hbar^2 / (2\mu_{2b} a^2)$. Weakly bound two-body dipolar states near an s-wave resonance ($a \gg D$) also exhibit this universal property. The binding energy for these states is shown in Fig. 1 (a) in units of the dipolar energy $E_D = \hbar^2 / \mu_{2b} D^2$ as a function of a/D . We have plotted the binding energies for three different resonances, the

first (black circles), second (blue diamonds) and eighth (red squares) resonance. As expected the three resonances agree very well in the large scattering length limit, but surprisingly the agreement is very good even when $a < D$.

To further illustrate universal features, we look at the partial wave populations as a function of a . We have numerically obtained the molecular wave function: $\psi_d(\vec{r}_{12}) = \sum_l Y_{l0}(\hat{r}_{12}) f_d^l(r_{12})$ where l is the partial wave. We require that $\sum_l N_l = 1$ where $N_l = \langle f_d^l | f_d^l \rangle$ is the partial wave population. Figure 1 (b) shows the s- (solid), d- (dashed), and g-wave (dotted) populations for the first (black) and second (blue) resonances as a function of a/D . This figure shows that the partial wave populations are universal. Additionally it shows that these molecules are mostly s- and d-wave. For large a , the s-wave contribution dominates and is near unity for large a and ψ_d takes on the universal form $r\psi_d \propto \exp(-r/a)$. As a is decreased the d-wave contribution becomes significant and reaches $\sim 40\%$. Even for very small a , the g-wave, i.e. $l = 4$, contribution is at most 2%. The dipolar interaction conserves parity and this selection rule prevents an s-wave channel coupling to any odd partial wave. This implies that the present theory applies to only bosonic or distinguishable dipoles.

There is of course a caveat to universality. The dipole length, D , must be much larger than any short range length scale, such as the depolarization, ‘‘dipole flip’’ length scale which is typically $100 a_0$ where a_0 is the Bohr radius [19]. At this point the short range physics will become important and the structure of the bound state will be system dependent. However, these results are widely applicable because the significant size of the dipolar length scale. It can easily reach $10^3 a_0$, some can even exceed $10^5 a_0$ for heavy, very polar molecules, such as LiCs.

To find the three-body recombination cross section we begin by considering three distinguishable dipoles and use a simple Fermi’s golden rule based approach which begins with the differential rate given by

$$dR = \frac{2\pi}{\hbar} |\langle \Psi_{2+1} | V | \Psi_{1+1+1} \rangle|^2 \delta(E_i - E_f). \quad (1)$$

Here the initial state, Ψ_{1+1+1} , is a three-body, box-normalized plane-wave in Jacobi coordinates. The final state, Ψ_{2+1} , consists of a weakly bound dimer and a box-normalized dipole-dimer plane wave. Because the dipole-dipole interaction has no diagonal s-wave contribution, we consider a modified two-body potential in Eq. (1) which incorporates the zero-range Fermi-pseudo potential to account for s-wave scattering, i.e.

$$V(\vec{r}) = \frac{d^2 [1 - 3(\hat{r} \cdot \hat{z})^2]}{r^3} + \frac{2\pi\hbar^2 a}{\mu_{2b}} \delta(\vec{r}). \quad (2)$$

where a is the positive s-wave scattering length near a dipole-dipole threshold scattering resonance and δ is the standard Dirac δ -function. Summing over all final-state

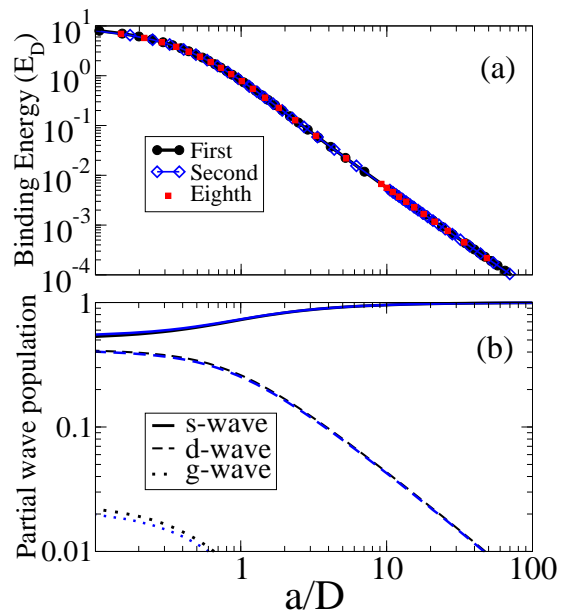


FIG. 1: (Color Online) Universal properties of 2 body dipolar scattering. (a) The binding energy (symbols with curves) of the dipolar dimer as a function of the s-wave scattering length. for the first (black circles), second (blue diamonds), and eighth (red square) resonance. (b) The partial wave molecular populations are shown for the s-wave (solid), d-wave (dashed) and g-wave (dotted) populations for the first (black) and second (blue) resonance.

energies and dividing by the total incident particle flux yields the total differential recombination cross section for three distinguishable dipoles [20],

$$\frac{d\sigma^{dist}}{d\hat{k}'_2} = \frac{\mu_{4b}^2 k'_2}{4\pi^2 \hbar^4 k} \left| \int d^3\rho_1 d^3\rho_2 \psi_d^*(\vec{\rho}_1) e^{-i\vec{k}'_2 \cdot \vec{\rho}_2} \times V(\vec{r}_{13}) e^{i(\vec{k}_1 \cdot \vec{\rho}_1 + \vec{k}_2 \cdot \vec{\rho}_2)} \right|^2. \quad (3)$$

Here $\vec{\rho}_i$ is a mass scaled Jacobi vector given by

$$\begin{aligned} \vec{\rho}_1 &= \sqrt{\frac{\mu_{12}}{\mu_{4b}}} (\vec{r}_1 - \vec{r}_2), \\ \vec{\rho}_2 &= \sqrt{\frac{\mu_{12,3}}{\mu_{4b}}} \left(\frac{\vec{r}_1 + \vec{r}_2}{2} - \vec{r}_3 \right), \\ \mu_{12} &= \frac{m_1 m_2}{m_1 + m_2}; \mu_{12,3} = \frac{(m_1 + m_2) m_3}{m_1 + m_2 + m_3}, \\ \mu_{4B} &= \sqrt{\frac{m_1 m_2 m_3}{m_1 + m_2 + m_3}}. \end{aligned}$$

In Eq. (3) \vec{k}'_2 is the outgoing dipole-dimer wave number with magnitude $k'_2 = \sqrt{2\mu_{4B}(E_{inc} + E_b)}$, $\vec{k}_{1(2)}$ is the incoming wave number associated with the first (second) Jacobi vector, $k = \sqrt{k_1^2 + k_2^2} = \sqrt{2\mu_{4B}E_{inc}}$ is the magnitude of the initial three-body plane wave with total incident energy E_{inc} . It should be noted that only a single two-body interaction is considered in Eq. (3). This is

the simplest matrix element that connects the outgoing dipole-dimer state to the incoming plane wave state.

Expanding the plane waves and dimer-wave function in Eq. (3) in spherical harmonics and integrating over the angular degrees of freedom yields the total distinguishable particle cross section:

$$\begin{aligned} \sigma^{dist} &= \frac{1024\pi^2}{3^{1/4}9\hbar k} \sqrt{mE_b} \quad (4) \\ &\times \sum_{L'l',Ll} \left| 4a\delta_{L'l'}\delta_{Ll0}\delta_{l0} (-1)^{l'} I_s^{l'} + DI_d^{L'l',Ll} \right|^2, \\ I_s^{l'} &= \int f_d^{l'*}(2R) j_{l'} \left(\sqrt{\frac{2\mu_{12,3}E_b}{\hbar^2}} R \right) R^2 dR, \\ I_d^{L'l',Ll} &= \int r^2 dr R^2 dR j_L \left(\sqrt{\frac{\mu_{12,3}}{\mu_{4B}}} k_2 R \right) j_l \left(\sqrt{\frac{\mu_{12}}{\mu_{4B}}} k_1 r \right) \\ &\times f_d^{l'*}(r) j_{l'} \left(\sqrt{\frac{2\mu_{12,3}E_b}{\hbar^2}} R \right) \left\langle L'l' \left| \frac{V_d(\vec{r}_{13})}{d^2} \right| Ll \right\rangle_{\Omega}. \end{aligned}$$

Here j_L is a spherical Bessel function, L and l are the initial angular momentum quantum numbers associated with the first and second Jacobi vectors respectively, L' is the angular momentum of the outgoing dipole-dimer system, and l' is the angular momentum of the dimer. We note that we have moved to standard Jacobi coordinates in these integrals for ease of calculations, i.e. $R = \sqrt{\mu/\mu_{12,3}}\rho_2$ and $r = \sqrt{\mu/\mu_{12}}\rho_1$. The $\delta_{Ll0}\delta_{l0}$ in Eq. (4) is due to the strong suppression all incoming angular momenta greater than zero in s-wave scattering. The expectation value $\langle L'l' | V_d(\vec{r}_{13}) | Ll \rangle_{\Omega}$ is only over all angular coordinates. The cross section in Eq. 4 was found by summing over all final outgoing momenta, \hat{k}'_2 , and averaging over all incoming directions $\{\hat{k}_1, \hat{k}_2\}$ as would be appropriate for a gas phase experiment.

The interaction in Eq. (3) is most easily evaluated with a biharmonic expansion [21], and it can be written as: $\frac{Y_{20}(\Omega_{12})}{|\vec{r}_1 - \vec{r}_2|^3} = \frac{1}{r_>} \sum_{kmm'} \left(\frac{r_<}{r_>} \right)^k [Y_{km}(\Omega_<) \otimes Y_{k+2m'}(\Omega_>)]_2^{(0)}$ where $r_>$ ($r_<$) is the greater (lesser) of r_1 and r_2 and $[Y_{km} \otimes Y_{k+2m'}]_{20}$ is a rank 2 tensor formed by the two spherical harmonics. This can then be evaluated by considering channels made up of two sets of partial wave, one for both \hat{r}_1 and \hat{r}_2 .

With this long range interaction one might expect that all partial waves contribute equally to the recombination process as is the case in two-dipole elastic scattering. This does not occur for the three-body inelastic scattering process. As long as the incoming particles are in the threshold regime, $E_{inc} \ll E_b$, all non-s-wave incoming channels are suppressed. This means that the final sum can be taken with zero initial angular momentum, $L = l = 0$, greatly simplifying the expression.

The final identical boson cross section σ^{ident} is found simply by multiplying by the Bose enhancement factor, $3!$, and restricting the sum in Eq. (4) to outgoing channels with the appropriate bosonic symmetry [22]. The

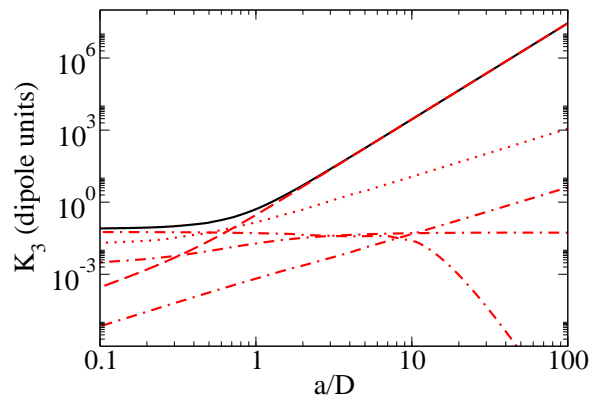


FIG. 2: (Color Online) The three-body recombination rate of three identical bosonic dipoles is shown in dipole units as a function of the scattering length. The total recombination rate (solid curves) is universal and independent of the resonance used. The sS (dashed red), dS (dotted red) and higher order (dot-dashed red curves) partial wave contributions are shown as well.

incoming channel is restricted to s-wave only and already obeys the appropriate symmetry. The recombination rate can be extracted from the inelastic cross section by multiplying by the characteristic incoming velocity $v = \hbar k / \mu_{4B}$ [10, 22]:

$$\begin{aligned} K_3^{ident} &= \frac{\hbar k}{\mu_{4B}} \sigma^{ident} = \frac{3! \sqrt{mE_b}}{m} \frac{1024 \sqrt{3} \pi^2}{3^{1/4} 9} \quad (5) \\ &\times \sum_{L'l'} \left| 4a\delta_{L'l'} I_s^{l'} + DI_d^{L'l',00} \right|^2. \end{aligned}$$

In general the integrals in Eq. (5) must be performed using numerically tabulated dimer wave functions $f_d^{l'}(r)$, but in the case where $a \gg D$ Fig. 1 (b) shows that the dipolar wave function is dominated by the s-wave component. Furthermore the wave function has the universal form for a weakly bound s-wave dimer: $\psi_d(\vec{r}) \rightarrow e^{-r/a} / (r\sqrt{2\pi a})$. Inserting this into Eq. (5) yields the large a scaling of the recombination rate:

$$\begin{aligned} K_3^{ident} &\rightarrow 3! \frac{32\sqrt{3}\pi^2 \hbar a^2}{m} [a^2 + \beta D^2], \quad (6) \\ \beta &= \frac{64}{15} (2\sqrt{3} - \pi)^2 = 0.44. \end{aligned}$$

The leading order a^4 term in this is exactly that found in Ref. [22, 23] for identical bosons with short-range s-wave interactions with the appropriate scattering matrix element set to $(ka)^4$. The second term is due entirely to the presence of the dipolar interaction and corresponds to an outgoing d-wave differential cross section. It should be noted that higher partial wave contributions in the dimer wave function are present at the $a^2 D^2$ order as well, but this contribution is two orders of magnitude smaller.

The results of the Fermi gold rule calculations are shown in Fig. 2 as a function of scattering length for

the first resonance in Fig. 1. The total rates have the expected a^4 scaling at large a due to the contact interaction, but as a/D is decreased a due to the contact interaction, but as a/D is decreased they eventually flatten out and when $D > a$ the rate is entirely controlled by the dipolar interaction, scaling as D^4 : $K_3^{ident} \rightarrow 0.079\hbar D^4/\mu_{2b}$. We have compared the recombination rates for several two-body resonances and have found nearly perfect agreement, to within $\sim 1\%$, indicating that the three-body recombination behavior found here is universal.

The dipolar interaction directly couples the incident channel to final states with $L' = 0, 2, 4, \dots$ and a molecular state with $l' = 0, 2, \dots$. The largest term in the $a > D$ regime, $l'L' = sS$ (dashed red curve), comes from the contact interaction and scales as a^4 . The next largest contribution from the sD channel (dotted red curve) scales as D^2a^2 . Additional contributions from higher order $l'L'$ channels are shown (dot-dashed red), but contribute little in the large a regime. However in the $a < D$ regime, the dominant contribution come from the $l'L' = dS$ and dG terms, the first of which is only weakly dependent on the scattering length. As one might expect there are two universal regimes that appear. The first regime appears where the long-range dipole interactions is dominant and the scattering length is small, i.e. $a \ll D$, where K_3 is independent of a and scales as D^4 . The second regime appears when a is the dominant length scale, $a \gg D$, and the a^4 s-wave contribution is dominant over all others.

The Fermi's golden rule based approach is only capable of describing the scaling behavior of three-body recombination, and does not incorporate more complex three-body correlations. The recombination rate can have a variety of interesting resonant behaviors on top of the envelope behavior presented here. For instance we ex-

pect that in the $a \gg D$ regime, a geometrically spaced set of Efimov minima are likely to appear in the $l'L' = sS$ outgoing channel [4].

We have shown the universal structure of weakly bound two-dipole states that depend only on the scattering length of the system, shown in Fig. 1. This has allowed us to obtain threshold three-body recombination rates into weakly-bound dimer states as a function of a . We used a Fermi Golden rule analysis to estimate the contributions to the rate from different events mediated by the dipole-dipole interaction and a contact interaction. These rates are shown in Fig. 2. The individual terms have many different scaling behaviors. When $a > D$, we find the dominant term scales as a^4 . When $D > a$ the recombination rate scales as D^4 . The case of negative scattering length is not addressed in this work, but it is not unreasonable to expect that the envelope behavior will be similar to that presented here. More detailed three-body calculations which include extra resonance structures are the subject of future work. The $|a| \gg D$ regime might also hold a variety of interesting phenomena such as universal three-dipole Efimov states.

Acknowledgments

The authors would like to thank H.R. Sadeghpour for numerous helpful discussions. Both authors gratefully acknowledge support from the NSF through ITAMP at Harvard University and Smithsonian Astrophysical Observatory. C.T. gratefully acknowledges partial support from the Australian Research Council and Los Alamos National Laboratory is operated by Los Alamos National Security, LLC for the NNSA of the USDoE under Contract No. DE-AC52-06NA25396.

-
- [1] S. Giorgini, L. P. Pitaevskii, and S. Stringari, *Rev. Mod. Phys.* **80**, 1215 (2008).
 - [2] Tin-Lun Ho, *Phys. Rev. Lett.* **92**, 090402 (2004).
 - [3] H. Hu, P. D. Drummond, and X.-J. Liu, *Nature Phys.* **3**, 469 (2007).
 - [4] For a review see: E. Braaten and H.-W. Hammer, *Phys. Rep.* **428**, 259 (2006); F. Ferlaino and R. Grimm, *Physics* **3**, 9 (2010).
 - [5] T. Kraemer *et al.*, *Nature* **440**, 315 (2006); S. Knoop *et al.*, *Nat. Phys.* **5**, 227 (2009).
 - [6] M. Zaccanti *et al.*, *Nat. Phys.* **5**, 586 (2009).
 - [7] S. E. Pollack, D. Dries, R. G. Hulet, *Science* **326**, 1683 (2009).
 - [8] V. Efimov, *Phys. Lett.* **33B**, 563 (1970); .
 - [9] T. Koehler, K. Goral, and P. S. Julienne *Rev. Mod. Phys.* **78**, 1311 (2006); C. Chin, *et al.*, *Rev. Mod. Phys.*, in press.
 - [10] P. O. Fedichev, M. W. Reynolds, and G. V. Shlyapnikov, *Phys. Rev. Lett.* **77**, 2921 (1996).
 - [11] K.-K. Ni, *et al.*, *Science* **322**, 231 (2008).
 - [12] S. Ospelkaus, *et al.*, *Science* **327**, 853 (2010).
 - [13] K.-K. Ni, *et al.*, arXiv:1001.2809.
 - [14] M. Marinescu and L. You, *Phys. Rev. Lett.* **81**, 4596 (1998).
 - [15] V. Roudnev and M. Cavagnero, *Phys. Rev. A* **79** 014701 (2009).
 - [16] C. Ticknor and J. L. Bohn *Phys. Rev. A* **72**, 032717 (2005).
 - [17] C. Ticknor, *Phys. Rev. Lett.* **100** 133202 (2008); *Phys. Rev. A* **76**, 052703 (2007).
 - [18] J. L. Bohn, M. Cavagnero, and C. Ticknor, *N. J. Phys.* **11** 055039 (2009).
 - [19] V. Roudnev and M. Cavagnero, *J. Phys. B* **42**, 044017 (2009).
 - [20] N. F. Mott and H. S. W. Massey, *Theory of Atomic Collisions*, Clarendon Press, Oxford 1965.
 - [21] A. Varshalovich, A.N. Moskalev, and V.K. Khersonskii, *Quantum Theory of Angular Momentum*, World Scientific Pub., 1988.
 - [22] B. D. Esry, C. H. Greene and J. P. Burke, *Phys. Rev. Lett.* **83**, 1751 (1999).
 - [23] N. P. Mehta, S. T. Rittenhouse, J. P. D'Incao, J. von Stecher, and Chris H. Greene, *Phys. Rev. Lett.* **103**, 153201 (2009).